Appl. Phys. A (2015) 118:479–486
DOI 10.1007/s00339-014-8794-4

Applied Physics A
Materials Science & Processing

Nitrogen-related changes in exciton localization and dynamics in GaInNAs/GaAs quantum wells grown by metalorganic vapor phase epitaxy

M. Baranowski · R. Kudrawiec · J. Misiewicz · M. Hammar

Received: 25 April 2014 / Accepted: 18 September 2014 / Published online: 1 October 2014
© The Author(s) 2014. This article is published with open access at Springerlink.com

Abstract In this work, we show the results of low-temperature photoluminescence (PL), time-resolved photoluminescence, and photoreflectance (PR) investigations, performed on a series of three $Ga_{0.64}In_{0.34}As_{1-x}N_x$/GaAs single quantum wells (SQW) grown by metalorganic vapor phase epitaxy with the nitrogen content of 0, 0.5, and 0.8 %. Comparing the PL and PR data, we show that at low excitation intensity and temperature, the radiative recombination occurs via localizing centers (LCs) in all samples. The excitation intensity-dependent PL measurements combined with theoretical modeling of hopping excitons in this system allow us to provide quantitative information on the disorder parameters describing population of LCs. It has been found that the average energy of LCs increases about two times and simultaneously the number of LCs increases about 10 and 20 times after the incorporation of 0.5 and 0.8 % of nitrogen, respectively. The value of average localization energy ε_0 determined for N-containing samples ($\sim$6–7 meV) is in the range typical for dilute nitride QWs grown by molecular beam epitaxy (MBE). On the other hand, the "effective" concentration of LCs seems to be higher than for GaInNAs/GaAs QW grown by MBE. The dramatic increase in localizing centers also affects the PL dynamics. Observed PL decay time dispersion is much stronger in GaInNAs SQW than in nitrogen-free SQW. The change in PL dynamic is very well reproduced by model of hopping excitons.

M. Baranowski (✉) · R. Kudrawiec · J. Misiewicz
Institute of Physics, Wroclaw University of Technology, Wybrzeze Wyspianskiego 27, 50-370 Wrocław, Poland
e-mail: michal.baranowski@pwr.wroc.pl

R. Kudrawiec
e-mail: robert.kudrawiec@pwr.wroc.pl

M. Hammar
Department of Microelectronics and Information Technology, Royal Institute of Technology (KTH), Electrum 229, 16440 Kista, Sweden

1 Introduction

III–V semiconductors with small amount of nitrogen (so-called dilute nitrides) such as GaNAs, GaInNAs, GaNAsSb, or InNAs are under great interest of scientists since last decade due to their unusual physical properties [1–3] and potential applications in near [1, 4–10] and mid-infrared [11–15] emitters, solar cells [16–20], and saturable absorber mirrors [21–25]. The most interesting feature of dilute nitrides is that the incorporation of small amount of nitrogen into III–V host causes a significant narrowing of the energy gap with the simultaneous reduction in the lattice constant [1]. This feature open up new possibilities in semiconductor band gap engineering and is especially attractive for construction of vertical cavity surface emitting laser based on GaAs. However, the structural and optical quality of dilute nitrides strongly deteriorate due to nitrogen incorporation, which is mainly caused by the ion-induced damage [26–28] or the incorporation of N atoms into interstitials [29–31] and local band gap fluctuation connected with different nitrogen neighborhood configurations in the GaInAsN alloys [32–35]. The deterioration of optical quality can be observed in low-temperature photoluminescence (PL) measurements. Usually, the PL spectra are very broad and asymmetric, and the temperature dependence of PL peak energy exhibits a deviation from Varshni's formula, i.e., so-called S shape [36–39]. The large broadening of the PL band and the S-shaped behavior are usually explained by the recombination of excitons localized on some potential fluctuations [38, 40–42]. The

origin of this localization effects can be related to quantum dot-like compositional fluctuations [43] or to deep donor-/acceptor-like states related to some point defects present after nitrogen incorporation [44, 45]. Also the kinetic properties of PL are affected by the localizing states, i.e., a spectral dispersion of PL decay time is observed [39, 46, 47].

So far, most of the investigations concerning optical properties of dilute nitride quantum wells (QWs) and layers have been performed on samples grown by MBE technique. The growth of dilute nitrides by MOVPE seems to be more challenging due to the lack of nitrogen source which is effectively decomposed and incorporated into the GaInNAs at relatively low temperature [48]. On the other hand, these growth methods are cheaper and faster than MBE which can be very important taking into account the increasing interest in the application of dilute nitrides in solar cells. Due to those advantages of MOVPE technique, some attempts to improve optical quality of QW grown by MOVPE have been done. Moreover, it has been shown that the quality of sample grown by MOVPE can be comparable to MBE samples [31, 49–53]. However, the optical properties of dilute nitrides material have been mainly studied for structures grown by MBE. There are very few work which somehow concern PL dynamics of GaInNAs material grown by MOVPE [46, 48] comparing to those grown by MBE [38, 47, 54–60].

In this work, we show the results of low-temperature PL, time-resolved photoluminescence (TRPL), and photoreflectance (PR), performed on a series of three $Ga_{0.64}In_{0.34}As_{1-x}N_x$/GaAs single quantum wells (SQWs) with the nitrogen concentration of 0, 0.5, and 0.8 %. Presented results of experimental measurements are supported by the simulation via model of hopping excitons. The combination of excitation intensity-dependent PL measurements with theoretical simulations enables us to determine the concentration of localizing centers (LCs) for different nitrogen content, relatively to nitrogen-free samples. Additionally, we compare the concentration of LCs with the date obtained for samples grown by MBE. Moreover, founded changes of LCs allow us to explain N-related changes in PL dynamics and observed dispersion of PL decay times.

2 Structure description and experimental details

$Ga_{0.64}In_{0.34}As_{1-x}N_x$/GaAs SQWs were grown by low-pressure (100 mbar) MOVPE on semi-insulating (001)-oriented GaAs substrates. The GaInAsN and GaInAs layers were grown at 515 and 540 °C, respectively, using triethylgallium, trimethylindium, dimethylhydrazine, and tertiarybutylarsine as precursors. The structures were capped with 100-nm-thick GaAs and subjected to an in situ annealing in AsH_3 ambient for 10 min at 680 °C. We have investigated three samples with QW thickness of 65 Å and nitrogen mole fractions equal to zero (the reference GaInAs/GaAs QW sample), 0.005 and 0.008, respectively [61]. To determine the N and In concentrations, the high-resolution X-ray diffraction investigations of the samples have been performed.

For all spectroscopic experiments, samples were held in vapor helium cryostat, which allows to perform measurements at 10 K. Photoreflectance (PR) experiment was performed with a tungsten halogen lamp (150 W) as a probe source. For photomodulation, a 632-nm line of He–Ne laser with 0.1 mW intensity was used as a pump beam that was mechanically chopped at frequency of 218 Hz. The probe and pump beams were focused to the diameter of 1 mm. A single grating 0.55-m monochromator and a thermoelectrically cooled GaInAs pin photodiode were used to analyze the reflected light. Other details of PR setup can be found in Ref [62]. For the PL and TRPL experiment, samples were excited by a mode-locked Ti:sapphire laser with 76 MHz repetition rate and a pulse duration of 150 fs. The average intensity of the pulsed laser beam used in the experiments was 2 mW. The laser beam was focused on the sample to a spot diameter of $\sim$0.2 mm. The PL signal was dispersed by a 0.3-m-focal length monochromator and detected by InGaAs linear array detector. The temporal evolution of PL has been detected by S1 InGaAs streak camera with the time resolution of about 25 ps.

3 Theoretical model

The carrier dynamics in dilute nitrides can be very well described within the model of hopping excitons [40–42, 58, 63–65]. So far, simulations of excitons hopping were mostly performed using the Monte Carlo approach. In the most basic approach, the dynamics of single exciton is simulated [40–42]; however, some modification in the Monte Carlo approach can be made in order to take into account different number of photogenerated excitons [58, 63, 65, 66]. In general, it was shown that the Monte Carlo approach successfully describes many characteristic features of PL in dilute nitrides such as the temperature dependence of PL peak position (i.e., so-called S shape of PL peak) and the dispersion of PL decay time [40, 42, 58, 64]. Recently to make the model of hopping excitons closer to realistic experimental conditions (i.e., to take into account a large number of excitons during the sample excitation without any simplification), we have proposed to solve directly the system of differential equations describing dynamics of excitons in GaInNAs/GaAs QWs

[67]. The advantage of this method is that the number of initially injected excitons can be easily changed without any simplification. This aspect is very important when the model is applied to explain the TRPL and intensity-dependent experiment where the number of initially photogenerated excitons can be very high due to the pulsed excitation. This simulations approach is in detail described in ref [67], so here we just briefly describe the most important parameters.

In this model, it is assumed that excitons behave like non-interacting single particles that can be trapped by localization potentials. At the beginning, energy of the localized states was chosen to create an exponential density of states (DOS): $DOS(\varepsilon) = \frac{N/L^2}{\varepsilon_0}\exp\left(-\frac{\varepsilon}{\varepsilon_0}\right)$, where L is the size of rectangle volume, N is the number localized centers in this volume, ε_0 is a characteristic energy of the localized centers distribution, and ε is a localization energy. In this work, the system of rate equations is solved for the randomly generated population of LCs. These simulations are repeated many times for different populations of LCs in order to imitate conditions which take place in our experiment where a large area of sample is excited. An exciton trapped by the localization states can recombine radiatively with the rate given by the inverse of it lifetime $v_r = \tau_r^{-1}$, hop to the mobility edge with rate given by $v_a = v_0 \exp(-\varepsilon/k_b T)$, or hop from localization state i to j with rate described by Miller–Abrahams formula $v_{ij} = v_0\left(-\frac{2r_{ij}}{\alpha} - \frac{\varepsilon_j-\varepsilon_i+\left|\varepsilon_j-\varepsilon_i\right|}{2kT}\right)$, v_0 is the attempt to escape frequency. Those excitons which are activated to the mobility edge can be again captured by not occupied localizing center. Carrier dynamics predicted by the model is determined by the dimensionless parameters $\tau_r v_o$ and $\alpha^2 N/L^2$, while the average energy of LCs ε_0 determines the full width of half maximum (FWHM) of the PL peak (FWHM $\approx 3\varepsilon_0$) [66, 68]. The α^2N^2/L^2 parameter describes the coupling strength between localizing states. This parameter increases with the density of LCs. For dilute nitrides grown by MBE, it was observed/assumed that this parameter is in the range of ~0.1–1 [41]. The parameter $\alpha^2 N/L^2$ can be also treated as an "effective" density of LCs. $\alpha^2 N/L^2$ can be also extracted from experimental data (see e.g., Ref [58]). In general, it is rather hard to get information about the absolute density of LCs from these simulations due to the lack of knowledge about the decay length α of wave function for localized excitons. Some estimation of LCs concentration could be made from the results of μ-PL and near field measurements presented in the literature [43–45]. From the results presented in abovementioned papers, the density of localized centers is in the range of few tens to about 100 localization states per μm^3. However, this is very rough estimation and its rather impossible to reliable estimate the α parameters from available data. It is important to note that due to hopping motion of excitons, the emission usually occurs from the locally deepest localizing states [65] and the amount of observed sharp lines in μ-PL or near field spectroscopy does not need to correspond to the amount of localizing states. For example, amount of sharp lines visible in μ-PL spectra depends on the excitation power [44]. Despite this, if we analyze a set of samples including reference sample (N-free sample for example), we are able to determine relative changes of LCs concentration after incorporation of different amount of nitrogen.

4 Results and discussion

4.1 Intensity-dependent measurements

Figure 1 shows results of PR measurements (open squares) together with normalized PL spectra measured for different excitation intensity changing from 1 to 30 mW at 10 K. The energy of free-excitonic transition for the three samples can be determined from PR measurements since this technique is not sensitive to localized states due to its absorption-like character [61]. This energy has been extracted from the fit of experimental data by Aspnes formula [65] and is marked by arrows in Fig. 1. It is clearly visible that the energy of ground state transition decreases with the rise of nitrogen concentration. At the same time at low excitation intensity, the PL emission from N-containing samples is clearly redshifted comparing to the energy of free-exciton transition determined from PR. The observed Stokes shift is a clear evidence of exciton localization in these QWs. A small Stokes shift is observed for N-free SQW at very low excitation conditions. It means that the effect of exciton localization is also present for N-free SQW, but its magnitude is weak. The dependence of Stokes shift versus nitrogen concentration for the excitation intensity of 1 mW is presented in Fig. 2a. The absolute value of Stokes shift increases with the increase in nitrogen concentration from ~1.5 meV for N-free SQW to ~23 meV for the SQW containing 0.8 % of nitrogen. Simultaneously, the broadening of PR resonance and PL peak increases with the increase in nitrogen concentration (see Fig. 2b). The increase in Stokes shift is directly connected with the N-related increase in concentration of LCs and average energy of LCs distribution [41, 58, 69]. So far, to the best of our knowledge, there is one article which describes the population of LCs in quantitative manner by means of hopping excitons model [41]. However, there are no systematic studies regarding the increase in LCs number due to nitrogen incorporation. Moreover, the results reported in Ref [39] are for samples grown by MBE, and it

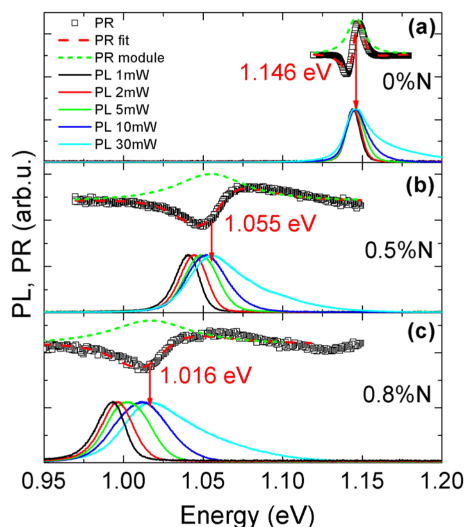

Fig. 1 PR spectra (*open squares*) of $Ga_{0.64}In_{0.34}As_{1-x}N_x$/GaAs SQW with the nitrogen concentration of 0 % (**a**), 0.5 % (**b**), and 0.8 % (**c**) together with normalized PL spectra obtained at different excitation intensity. *Dashed red lines* are fit curves of PR data, and *green short-dash lines* are modules of PR resonance. *Arrows* indicate the energy of free-exciton transition for each SQW

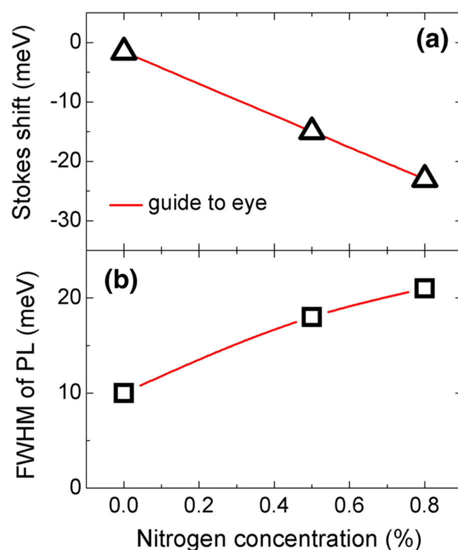

Fig. 2 **a** Value of Stokes shift obtained at the excitation intensity of 1 mW and **b** FWHM of PL peak for $Ga_{0.64}In_{0.34}As_{1-x}N_x$/GaAs SQW with different nitrogen concentration

is interesting to evaluate and compare parameters describing the population of LCs in GaInNAs/GaAs SQW samples grown by MOVPE technique.

To evaluate the N-related changes in concentration of LCs in GaInNAs/GaAs SQW samples, we have performed PL measurements for various intensity excitation condition and applied the model of hopping excitons. With the increase in excitation intensity, we expect that the absolute value of Stokes shift should decrease due to the saturation

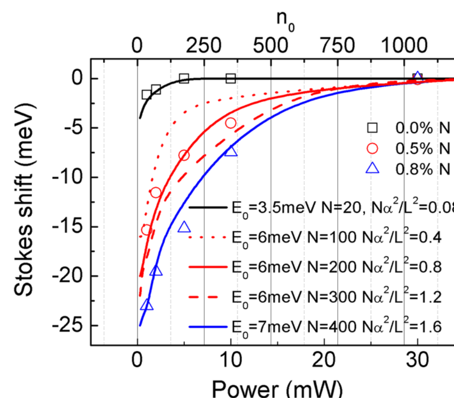

Fig. 3 Dependence of Stoke shift as a function of excitation intensity for $Ga_{0.64}In_{0.34}As_{1-x}N_x$/GaAs SQW containing 0 % (*open black squares*), 0.5 % (*open red circles*), and 0.8 % (*open blue triangles*). The *solid lines* show the best fits of the excitation dependence of Stoke shift obtained by the simulation. The *dotted* and *dashed lines* are examples of simulated Stokes shift dependence for other concentrations of LCs

of LCs. Obviously, the saturation of LCs should occur faster for structures with lower concentration of LCs. Figure 3 shows the dependence of Stoke shift as a function of excitation intensity, (see open squares, circle, and triangles). It can be seen that for N-free sample (open squares), the total saturation of LCs (no Stokes shift) occurs when the excitation intensity is 5 mW, while for N-containing samples the excitation intensity has to be as high as 30 mW. The dependence of Stokes shift for the three SQW structures can be very nicely reproduced within the model of hopping excitons, and hence, parameters describing the population of LCs can be extracted.

In order to determine N-related changes in concentration of LCs for this set of SQW samples, we applied the according approach with following assumptions. Based on the previous works [68, 69], it is assumed that the FWHM of the PL peak at low excitation condition depends only on the ε_0 parameter. Thus, the FWHM is insensitive to the change of α^2N^2/L^2, and the value of ε_0 can be determined according to the rule FWHM $\approx 3\varepsilon_0$. In our case, it leads to an average energy of LCs which equals 3.5, 6.0, and 7.0 meV for the sample with 0, 0.5, and 0.8 % of N, respectively. The redshift of the PL peak depends on both ε_0 (determined from FWHM) and α^2N/L^2 as well as initial amount of excitons n_0 injected into the structure. In order to estimate the value of α^2N/L^2 for each SQW, we have performed simulation of PL spectra with the determined value of ε_0, different values of initially injected excitons n_0, and various numbers of LCs, i.e., various N. From this simulation, we have extracted the dependence of Stokes shift vs. n_0 for different values of α^2N/L^2. Finally, we found scaling parameter between the n_0 and the excitation intensity. It enables us to fit the excitation intensity

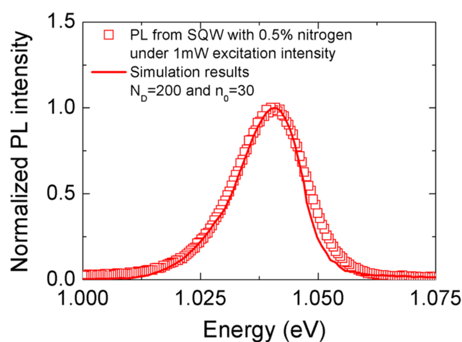

Fig. 4 Example of measured PL spectra (*open squares*) obtained from $Ga_{0.64}In_{0.34}As_{0.995}N_{0.005}/GaAs$ SQW under 1 mW excitation intensity together with simulated PL spectra (*solid line*)

dependence of Stoke shift by the simulated curves. The results of this analysis are presented in Fig. 3 by the solid lines. An example of simulated PL spectra is presented in Fig. 4 together with the measured PL. Very good agreement between simulations and experimental results is visible on both figures. We also add some plots (dotted and dashed lines) of simulated dependence of Stoke shift for $\varepsilon_0 = 6$ meV and different value of $\alpha^2 N/L^2$ which shows that the choice of this parameters is unique.

The values of all important parameters used in our simulations are summarized in Table 1. Moreover, the values of parameters describing the average energy ε_0 and the relative concentration of LCs are also shown in Fig. 5a, b. It can be seen that the incorporation of 0.8 % nitrogen causes an increase in the ε_0 from 3.5 to 7.0 meV. However, these changes are not so dramatic as the N-related increase in the density of LCs. The concentration of LCs after incorporation of 0.5 and 0.8 % of nitrogen increase about 10 and 20 times, respectively (comparing to nitrogen-free sample). This huge increase in concentration of LCs explains why all effects connected with the carrier/exciton localization are so commonly observed in structures based on dilute nitrides. It is worth noting that the increase in concentration of LCs causes that it is harder to saturate them and makes the hopping transfer between different LC states more probable. At the same time, we need to be aware that the hopping process is essential for all the characteristic behavior of low-temperature PL such as S shape [40, 41] of PL, decay time dispersion of PL [58, 64, 67], and sharp lines in μ-PL spectra [65, 66]. The value of ε_0 determined for N-containing samples (6–7 meV) is in the range, which is typical for “standard” dilute nitride quantum wells grown by MBE [41, 58] (quantum well width in the range of 6–7.5 nm, indium content 20–38 %, and nitrogen content 0.5–3 %). On the other hand, the “effective” concentration $\alpha^2 N/L^2$ seems to be higher than for similar samples grown by MBE, for which $\alpha^2 N/L^2$ is in the range of 0.1–1 [41, 58].

Table 1 Value of essential parameters used in simulations

N (%)	τ_r (ns)	ν_0 (ns^{-1})	N	$N(\alpha/L)^2$	ε_0 (meV)
0	0.5	1,000	20	0.08	3.5
0.5	0.5	1,000	200	0.8	6
0.8	0.5	1,000	400	1.6	7

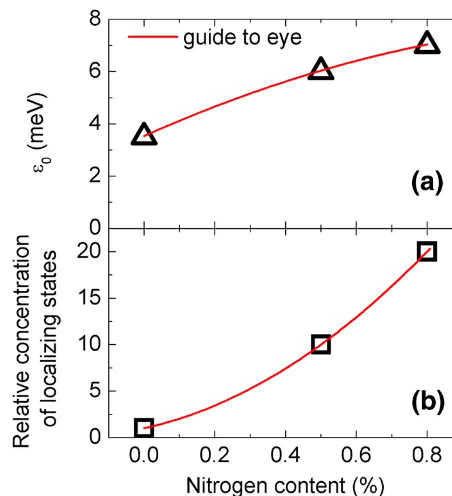

Fig. 5 N-related dependence of average localization energy ε_0 (**a**) and “effective” concentration $\alpha^2 N/L^2$ of LCs (**b**)

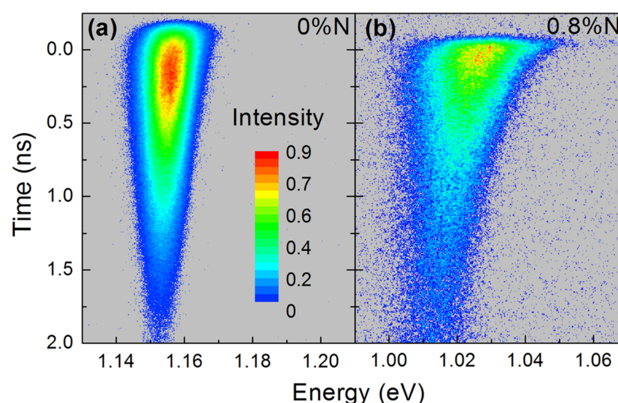

Fig. 6 Temporal evolution of PL spectrum (i.e., streak image) obtained at 10 K for $Ga_{0.64}In_{0.34}As_{0.995}N_{0.005}/GaAs$ SQW containing 0 % (**a**) and 0.8 % (**b**) nitrogen

4.2 Time-resolved photoluminescence

In the context of such dramatic increase in concentration of LCs, it is interesting to study how this affects the excitons dynamics in the investigated series of SQW. Figure 6a, b shows the temporal evolution of PL spectrum (i.e., streak image) of N-free and N-containing QW. It is clearly visible that due to incorporation of nitrogen into InGaAs QW, the PL peak is broader and has stronger asymmetry, and decay time of PL signal varies strongly with the spectral position.

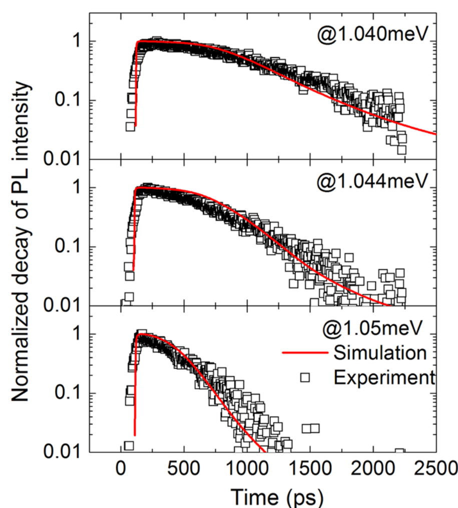

Fig. 7 Examples of PL decay curves (*open squares*) obtained for different energy for $Ga_{0.64}In_{0.34}As_{0.995}N_{0.005}/GaAs$ SQW at the excitation intensity of 2 mW together with the simulated decays curves (*red solid lines*)

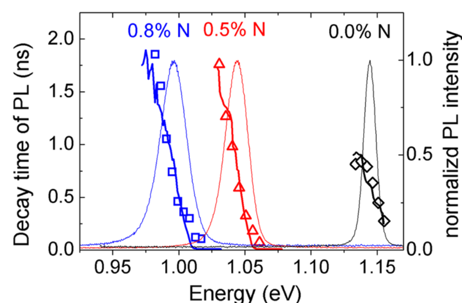

Fig. 8 Dispersion of PL decay time determined (*open points*) and simulated (*lines*) for $Ga_{0.64}In_{0.34}As_{0.995}N_{0.005}/GaAs$ SQWs together with normalized PL spectra

Figure 7 shows the examples of decays of PL (open squares) from QW sample with 0.5 % of nitrogen taken at different energy of detection. It is clearly visible that the decay time of PL depends on the detection energy, and this time is shorter on the high-energy side and longer on the low-energy side, i.e., a dispersion of PL decay time is observed for this sample.

Figure 8 shows the PL decay time determined at different energies for the three samples studied in this paper. For simplicity, we define the decay time as the time when the intensity of PL decrease *e* times from the maximum value. The dispersion of PL decay time is observed in all samples, but it is much stronger (in the sense of the difference of PL decay time at low- and high-energy side PL peak) for N-containing samples. This effect is directly connected with the concentration of LCs. The observed PL decay time dispersion is a result of excitons transfers via hopping process between different LCs. At low temperature, the values of τ_{PL} are reduced at higher energies since the exciton recombination dynamics is affected by the transfer of excitons to lower-energy states. Simultaneously, the exciton transfer from low-energy states to high-energy states is damped at low temperatures since excitons do not have sufficient thermal energy for such a transfer. The asymmetry between the exciton transfer process causes that the PL decay time at low-energy side is elongated due to refilling of low-energy LCs by relaxing excitons. The spectral dispersion of PL decay time is much stronger for N-containing samples due to more effective hopping process between LCs, i.e., LCs are closer to each other in N-containing samples because of their higher concentration in comparison with N-free sample. Results of theoretical simulations are presented together with experimental data in Figs. 7 and 8. The agreement between experiment and simulation performed with the parameters determined from intensity-dependent PL measurements is very good. The simulated temporal evolution of PL very well reproduces experimentally obtained decays of PL, as shown in Fig. 7. Moreover, the decay time dispersion is very well reproduced for the three samples, as shown in Fig. 8. This indicates that the dispersion of PL decay times is a result of exciton hopping from higher- to lower-energy LCs and the concentration of LCs affects the strength of this dispersion. For high concentration of LC states (samples with nitrogen), the dispersion strength stops to increase. This result is in agreement with our previous simulation [69] and is connected with the saturation of carrier transfer effectiveness.

5 Conclusion

In conclusion, PL, TRPL, and PR measurements have been performed for a series of $Ga_{0.64}In_{0.34}As_{1-x}N_x/GaAs$ SQW with different nitrogen concentration (0, 0.5, 0.8 %) grown by MOVPE. Comparing the PL and PR data at low temperatures, it has been shown that at low excitation intensity the radiative recombination occurs via LCs in all samples at low temperature. Analyzing the intensity-dependent PL measurements within the model of hopping excitons, the N-related changes in the average energy of LCs ε_0 and the relative concentration of LCs have been determined. The average energy of LCs rises about two times and simultaneously the number of LCs increases about 10 and 20 times after the incorporation of 0.5 and 0.8 % of nitrogen, respectively. This increase in concentration of LCs explains the observed changes in the Stokes shift and PL dynamics. The dispersion of PL decay times is much stronger for N-containing which is very well reproduced within the model of hopping excitons.

6 Acknowledgments

This work was performed within the Grant of the National Science Centre (No. 2012/07/E/ST3/01742). M. B. acknowledges support from the MNiSW within the Iuventus Plus Program (IP2011 001471).

Open Access This article is distributed under the terms of the Creative Commons Attribution License which permits any use, distribution, and reproduction in any medium, provided the original author(s) and the source are credited.

References

1. M. Kondow, K. Uomi, A. Niwa, T. Kitatani, S. Watahiki, Y. Yazawa, Jpn. J. Appl. Phys. **35**, 1273 (1996)
2. W. Shan, W. Walukiewicz, J.W. Ager, E.E. Haller, J.F. Geisz, D.J. Friedman, J.M. Olson, S.R. Kurtz, Phys. Rev. Lett. **82**, 1221 (1999)
3. I. Suemune, K. Uesugi, W. Walukiewicz, Appl. Phys. Lett. **77**, 3021 (2000)
4. M. Reinhardt, M. Fischer, M. Kamp, J. Hofmann, A. Forchel, IEEE Photonics Technol. Lett. **12**, 239 (2000)
5. W. Li, T. Jouhti, C.S. Peng, J. Konttinen, P. Laukkanen, E.-M. Pavelescu, M. Dumitrescu, M. Pessa, Appl. Phys. Lett. **79**, 3386 (2001)
6. W. Ha, V. Gambin, M. Wistey, S. Bank, S. Kim, J.S. Harris, IEEE Photonics Technol. Lett. **14**, 591 (2002)
7. S. Sato, S. Satoh, Electron. Lett. **34**, 1495 (1998)
8. K.H. Tan, S.F. Yoon, S. Fedderwitz, A. Stohhr, W.K. Loke, S. Wicaksono, T.K. Ng, M. Weiss, A. Poloczek, V. Rymanov, A.S. Patra, E. Tangdiongga, D. Jager, IEEE Electron Device Lett. **30**, 590 (2009)
9. K.H. Tan, S.F. Yoon, W.K. Loke, S. Wicaksono, K.L. Lew, A. Stöhr, O. Ecin, A. Poloczek, A. Malcoci, D. Jäger, Appl. Phys. Lett. **90**, 183515 (2007)
10. Z. Xu, N. Saadsaoud, M. Zegaoui, W.K. Loke, K.H. Tan, S. Wicaksono, S.F. Yoon, C. Legrand, D. Decoster, J. Chazelas, IEEE Electron Device Lett. **31**, 449 (2010)
11. A. Krier, M. de la Mare, P.J. Carrington, M. Thompson, Q. Zhuang, A. Patanè, R. Kudrawiec, Semicond. Sci. Technol. **27**, 094009 (2012)
12. Q. Zhuang, A. Godenir, A. Krier, G. Tsai, H.H. Lin, Appl. Phys. Lett. **93**, 121903 (2008)
13. M. de la Mare, P.J. Carrington, R. Wheatley, Q. Zhuang, R. Beanland, A.M. Sanchez, A. Krier, J. Phys. Appl. Phys. **43**, 345103 (2010)
14. R. Chen, S. Phann, H.D. Sun, Q. Zhuang, A.M.R. Godenir, A. Krier, Appl. Phys. Lett. **95**, 261905 (2009)
15. M. Latkowska, R. Kudrawiec, F. Janiak, M. Motyka, J. Misiewicz, Q. Zhuang, A. Krier, W. Walukiewicz, Appl. Phys. Lett. **102**, 122109 (2013)
16. N. López, L.A. Reichertz, K.M. Yu, K. Campman, W. Walukiewicz, Phys. Rev. Lett. **106**, 028701 (2011)
17. N. Ahsan, N. Miyashita, M.M. Islam, K.M. Yu, W. Walukiewicz, Y. Okada, IEEE J. Photovolt. **3**, 730 (2013)
18. K.H. Tan, S. Wicaksono, W.K. Loke, D. Li, S.F. Yoon, E.A. Fitzgerald, S.A. Ringel, J.S. Harris Jr, J. Cryst. Growth **335**, 66 (2011)
19. D.J. Friedman, J.F. Geisz, S.R. Kurtz, J.M. Olson, J. Cryst. Growth **195**, 409 (1998)
20. J.F. Geisz, D.J. Friedman, J.M. Olson, S.R. Kurtz, B.M. Keyes, J. Cryst. Growth **195**, 401 (1998)
21. A. Rutz, V. Liverini, E. Müller, S. Schön, U. Keller, J. Cryst. Growth **301–302**, 525 (2007)
22. S. Schön, A. Rutz, V. Liverini, R. Grange, M. Haiml, S.C. Zeller, U. Keller, J. Cryst. Growth **278**, 239 (2005)
23. S. Calvez, N. Laurand, H.D. Sun, J. Weda, D. Burns, M.D. Dawson, A. Harkonen, T. Jouhti, M. Pessa, M. Hopkinson, D. Poitras, J.A. Gupta, C.G. Leburn, C.T.A. Brown, W. Sibbett, Phys. Status Solidi A **205**, 85 (2008)
24. V. Liverini, S. Schön, R. Grange, M. Haiml, S.C. Zeller, U. Keller, Appl. Phys. Lett. **84**, 4002 (2004)
25. A. Khadour, S. Bouchoule, G. Aubin, J.-C. Harmand, J. Decobert, J.-L. Oudar, Opt. Express **18**, 19902 (2010)
26. W.K. Loke, S.F. Yoon, T.K. Ng, S.Z. Wang, W.J. Fan, J. Vac. Sci. Technol. B Microelectron. Nanometer Struct. **20**, 2091 (2002)
27. Z. Pan, L.H. Li, W. Zhang, Y.W. Lin, R.H. Wu, W. Ge, Appl. Phys. Lett. **77**, 1280 (2000)
28. J. Miguel-Sánchez, A. Guzmán, E. Muñoz, Appl. Phys. Lett. **85**, 1940 (2004)
29. S.G. Spruytte, C.W. Coldren, J.S. Harris, W. Wampler, P. Krispin, K. Ploog, M.C. Larson, J. Appl. Phys. **89**, 4401 (2001)
30. L. Li, Z. Pan, W. Zhang, Y. Lin, X. Wang, R. Wu, J. Cryst. Growth **227–228**, 527 (2001)
31. A.J. Ptak, S.W. Johnston, S. Kurtz, D.J. Friedman, W.K. Metzger, J. Cryst. Growth **251**, 392 (2003)
32. P.J. Klar, H. Grüning, J. Koch, S. Schäfer, K. Volz, W. Stolz, W. Heimbrodt, A.M.K. Saadi, A. Lindsay, E.P. O'Reilly, Phys. Rev. B **64**, 121203 (2001)
33. R. Kudrawiec, G. Sęk, J. Misiewicz, D. Gollub, A. Forchel, Appl. Phys. Lett. **83**, 2772 (2003)
34. V. Lordi, V. Gambin, S. Friedrich, T. Funk, T. Takizawa, K. Uno, J.S. Harris, Phys. Rev. Lett. **90**, 145505 (2003)
35. R. Kudrawiec, E.-M. Pavelescu, J. Andrzejewski, J. Misiewicz, A. Gheorghiu, T. Jouhti, M. Pessa, J. Appl. Phys. **96**, 2909 (2004)
36. R. Kudrawiec, G. Sęk, J. Misiewicz, L.H. Li, J.C. Harmand, Appl. Phys. Lett. **83**, 1379 (2003)
37. R. Kudrawiec, G. Sek, J. Misiewicz, L.H. Li, J.C. Harmand, Eur. Phys. J. Appl. Phys. **27**, 313 (2004)
38. I.A. Buyanova, W.M. Chen, G. Pozina, J.P. Bergman, B. Monemar, H.P. Xin, C.W. Tu, Appl. Phys. Lett. **75**, 501 (1999)
39. A. Kaschner, T. Lüttgert, H. Born, A. Hoffmann, A.Y. Egorov, H. Riechert, Appl. Phys. Lett. **78**, 1391 (2001)
40. S.D. Baranovskii, R. Eichmann, P. Thomas, Phys. Rev. B **58**, 13081 (1998)
41. O. Rubel, M. Galluppi, S.D. Baranovskii, K. Volz, L. Geelhaar, H. Riechert, P. Thomas, W. Stolz, J. Appl. Phys. **98**, 063518 (2005)
42. O. Rubel, S.D. Baranovskii, K. Hantke, B. Kunert, W.W. Rühle, P. Thomas, K. Volz, W. Stolz, Phys. Rev. B **73**, 233201 (2006)
43. A.M. Mintairov, T.H. Kosel, J.L. Merz, P.A. Blagnov, A.S. Vlasov, V.M. Ustinov, R.E. Cook, Phys. Rev. Lett. **87**, 277401 (2001)
44. M. Latkowska, R. Kudrawiec, G. Sęk, J. Misiewicz, J. Ibáñez, M. Henini, M. Hopkinson, Appl. Phys. Lett. **98**, 131903 (2011)
45. R. Kudrawiec, M. Latkowska, M. Baranowski, J. Misiewicz, L.H. Li, J.C. Harmand, Phys. Rev. B **88**, 125201 (2013)
46. R.A. Mair, J.Y. Lin, H.X. Jiang, E.D. Jones, A.A. Allerman, S.R. Kurtz, Appl. Phys. Lett. **76**, 188 (2000)
47. R. Kudrawiec, M. Syperek, M. Latkowska, J. Misiewicz, V.-M. Korpijärvi, P. Laukkanen, J. Pakarinen, M. Dumitrescu, M. Guina, M. Pessa, J. Appl. Phys. **111**, 063514 (2012)
48. K.-S. Kim, S.-J. Lim, K.-H. Kim, J.-R. Yoo, T. Kim, Y.-J. Park, J. Cryst. Growth **273**, 368 (2005)

49. N. Tansu, J.-Y. Yeh, L.J. Mawst, Appl. Phys. Lett. **83**, 2512 (2003)
50. G. Kolhatkar, A. Boucherif, C.E. Valdivia, S.G. Wallace, S. Fafard, V. Aimez, R. Arès, J. Cryst. Growth **380**, 256 (2013)
51. Z. Pan, T. Miyamoto, D. Schlenker, S. Sato, F. Koyama, K. Iga, J. Appl. Phys. **84**, 6409 (1998)
52. A. Yue, K. Shen, R. Wang, J. Shi, IEEE Photonics Technol. Lett. **16**, 717 (2004)
53. M. Kawaguchi, T. Miyamoto, E. Gouardes, T. Kondo, F. Koyama, K. Iga, Appl. Phys. Lett. **80**, 962 (2002)
54. X.D. Luo, J.S. Huang, Z.Y. Xu, C.L. Yang, J. Liu, W.K. Ge, Y. Zhang, A. Mascarenhas, H.P. Xin, C.W. Tu, Appl. Phys. Lett. **82**, 1697 (2003)
55. Z. Sun, Z.Y. Xu, X.D. Yang, B.Q. Sun, Y. Ji, S.Y. Zhang, H.Q. Ni, Z.C. Niu, Appl. Phys. Lett. **88**, 011912 (2006)
56. T.K. Ng, S.F. Yoon, S.Z. Wang, L.-H. Lin, Y. Ochiai, T. Matsusue, J. Appl. Phys. **94**, 3110 (2003)
57. I.A. Buyanova, G. Pozina, P.N. Hai, W.M. Chen, H.P. Xin, C.W. Tu, Phys. Rev. B **63**, 033303 (2000)
58. M. Baranowski, R. Kudrawiec, M. Latkowska, M. Syperek, J. Misiewicz, J.A. Gupta, Appl. Phys. Lett. **100**, 202105 (2012)
59. M. Baranowski, R. Kudrawiec, M. Syperek, J. Misiewicz, H. Zhao, M. Sadeghi, S.M. Wang, Semicond. Sci. Technol. **26**, 045012 (2011)
60. M. Baranowski, R. Kudrawiec, M. Latkowska, M. Syperek, J. Misiewicz, T. Sarmiento, J. S. Harris, J. Phys. Condens. Matter **25**, 065801 (2013)
61. R. Kudrawiec, G. Sęk, K. Ryczko, J. Misiewicz, P. Sundgren, C. Asplund, M. Hammar, Solid State Commun. **127**, 613 (2003)
62. R. Kudrawiec, J. Misiewicz, Rev. Sci. Instrum. **80**, 096103 (2009)
63. K. Jandieri, B. Kunert, S. Liebich, M. Zimprich, K. Volz, W. Stolz, F. Gebhard, S.D. Baranovskii, N. Koukourakis, N.C. Gerhardt, M.R. Hofmann, Phys. Rev. B **87**, 035303 (2013)
64. O. Rubel, W. Stolz, S.D. Baranovskii, Appl. Phys. Lett. **91**, 021903 (2007)
65. M. Baranowski, M. Latkowska, R. Kudrawiec, J. Misiewicz, J. Phys. Condens. Matter **23**, 205804 (2011)
66. M. Baranowski, M. Latkowska, R. Kudrawiec, J. Misiewicz, Acta Phys. Pol. A **120**, 899 (2011)
67. M. Baranowski, R. Kudrawiec, J. Misiewicz, Jpn. J. Appl. Phys. **52**, 08JL04 (2013)
68. H. Grüning, K. Kohary, S.D. Baranovskii, O. Rubel, P.J. Klar, A. Ramakrishnan, G. Ebbinghaus, P. Thomas, W. Heimbrodt, W. Stolz, W.W. Rühle, Phys. Status Solidi C **1**, 109 (2004)
69. M. Baranowski, R. Kudrawiec, M. Latkowska, M. Syperek, J. Misiewicz, Acta Phys. Pol. A **122**, 1022 (2012)